

Article

Calculation of the Mass Transfer Coefficient for the Dissolution of Multiple Carbon Dioxide Bubbles in Sea Water under Varying Conditions

Hee-Joo Cho and Jungho Choi * 

Department of Naval Architecture and Offshore Engineering, Dong-A University, 49315 Busan, Korea; ll5943@naver.com

* Correspondence: tamuchoi@dau.ac.kr

Received: 2 November 2019; Accepted: 11 December 2019; Published: 13 December 2019



Abstract: Underwater weapon systems with reforming fuel cells have been developed to increase the number of possible days that the former can be submerged. Reforming hydrocarbons generate a large quantity of carbon dioxide gas that must be completely dissolved in water and released. In this study, the mass transfer coefficient was derived experimentally while changing the process variables that affect mass transfer, such as bubble size, presence/absence of an inline mixer, retention time, pressure, and solvent type. It was found that retention time was most affected, followed by type of solvent, presence/absence of the inline mixer, and bubble size. In addition, by reducing bubble size and retention time and applying an inline mixer, the effect can be like that dissolved at high pressure even at low pressure. Applications of this study are expected to reduce the size of underwater weapon systems. Therefore, further studies on increasing the power consumption of underwater weapon systems due to reduction of bubble size and the application of inline mixers should be conducted.

Keywords: air independent propulsion system; underwater weapon system; hydrocarbon reforming; carbon dioxide; mass transfer; mass transfer coefficient; multiple bubble; dissolution

1. Introduction

Underwater weapon systems equipped with air independent propulsion (AIP) have been constructed recently to increase their submerged operation period [1]. AIP systems using reformed fuel cells, which supply hydrogen to fuel cells by reforming hydrocarbons, have the advantage of continuously producing more hydrogen compared to the metallic alloy currently used to store hydrogen [2]. However, reforming hydrocarbons has the disadvantage of generating a large amount of carbon dioxide [3]. The carbon dioxide generated in an underwater weapon system must be stored within the underwater weapon system itself or discharged outside. If the latter is done with no processing or refinement, the bursting bubbles generate noise that can be detected by opponents. Therefore, the carbon dioxide must be fully dissolved in the sea water before being discharged [4].

Many studies have been conducted on the dissolution and absorption of carbon dioxide. Harun et al. [5] modeled and compared the Mono Ethanol Amine (MEA) absorption process to capture carbon dioxide generated from coal-fired thermal power plants through dynamic simulation using Aspen Plus and gPROMS. Pao Chi Chen et al. [6] used a continuous bubble column scrubber to absorb carbon dioxide generated from coal-fired power plants. They evaluated the effects of operating temperature, pH, and gas-liquid flow on the carbon dioxide absorption efficiency and total mass transfer coefficient in a NaOH solution and derived the optimal design variables for the scrubber. To capture and store carbon dioxide in combustion gas generated from fossil fuel power plants, Mohammad et al. [7] evaluated the carbon dioxide removal rate while changing the MEA concentration,

stripper operation pressure, and operating temperature. Carderbank and Rochiel [8] experimented on mass transfer according to the size of single bubble. Liu et al. [9] researched the dissolution and diffusion of carbon dioxide in sea water and distilled water at various temperatures and pressures to store carbon dioxide in the ocean. In terms of carbon capture and storage (CCS) of combustion gas generated from power plants, most previous studies evaluated the carbon dioxide absorption rate using a chemical absorbent or researched the carbon dioxide dissolution characteristics in a single bubble. However, it is difficult to apply the results of previous studies here because the carbon dioxide generated from underwater weapon systems is under different temperature and pressure conditions than the carbon dioxide gas generated from power plants, further, for the weapon systems, the carbon dioxide rarely occur as single bubbles. Therefore, fully dissolving multiple carbon dioxide bubbles generated from an underwater weapon system in sea water with no chemical absorbent is very important for the safety and proper functioning of the weapons. In the present study, the dissolution characteristics of carbon dioxide were analyzed while changing the process variables that affect mass transfer and the optimal combination of process variables was derived.

2. Theory

Carbon dioxide is dissolved in water by the gas–liquid mass transfer phenomenon. To determine the rate of dissolution of carbon dioxide, it is essential to derive an appropriate gas–liquid mass transfer coefficient [10]. The mass transfer coefficient is an indicator for how quickly materials are diffused and transferred at the gas–liquid interface. Ranz and Marshall (1952) defined the mass transfer rate of a single bubble in liquid as follows [11]:

$$\dot{m} = A_b J_i = \pi d_b^2 \cdot k_i^l \cdot (C_i^{sol} - C_i^l), \tag{1}$$

where d_b is the diameter of the gas bubble, k_i^l is the mass transfer coefficient of gas bubble i in liquid, C_i^{sol} is the solubility of gas bubble i in liquid, and C_i^l is the concentration of gas bubbles in liquid. By applying Henry’s law on the solubility of gas bubbles, we can define the mass transfer rate as follows [12]:

$$\dot{m} = A_b J_i = \pi d_b^2 \cdot k_i^l \cdot (H_i P_i - C_i^l), \tag{2}$$

where P_i is the partial pressure of the gas bubble and H_i is the Henry constant of gas.

As can be seen from Equations (1) and (2), the mass transfer rate between gas and liquid is proportional to the bubble’s contact area, mass transfer coefficient, and concentration difference.

Wing and John [13] derived the diffusion coefficients of N_2 , O_2 , and CO_2 when the gas bubble size was constant in water at 25 °C. The rate of dissolution can be defined as Equation (3).

$$V = \frac{4\pi\alpha C_0 D}{\rho} \cdot t, \tag{3}$$

where C_0 is the initial concentration of the gas, D is the diffusion coefficient of the gas in the liquid, V is the rate of solution of the gas from the bubble. The rate of dissolution is proportional to the radius of bubble (α) and retention time (t).

Higbie [14] defined the mass transfer coefficient of pure gas as follows:

$$k = \frac{2}{\sqrt{\pi}} \sqrt{Re Sc} \frac{D}{d_b}, \tag{4}$$

$$Re = \frac{\rho_l d_b u_b}{\mu_l}, \tag{5}$$

$$Sc = \frac{\mu_l}{\rho_l D}, \tag{6}$$

where k is the mass transfer coefficient, Re is the Reynolds number, Sc is the Schmidt number, ρ_l is the density of liquid, u_b is the slip velocity of the bubble, and μ_l is the viscosity of the liquid.

The mass transfer coefficient is dependent on Reynolds number, Schmidt number, diffusivity, and bubble diameter.

Liu et al. [9] experimented on the dissolution and diffusion process of a single CO₂ bubble in sea water and pure water and found that the extinction speed of a bubble is faster if the pressure is higher, the solvent is pure water, and the initial bubble diameter is smaller. Carderbank et al. [8] derived the rate of solution, shape, and mass transfer coefficient of CO₂ bubbles in distilled water through experiments. These previous studies show that the variables affecting mass transfer include pressure, bubble size, retention time, concentration difference, and solvent type.

Therefore, in this study, the dissolution behavior of CO₂ was analyzed while changing the variables affecting mass transfer such as pressure, bubble size, retention time, concentration difference, and solvent type, and derived the mass transfer coefficient through experiments.

3. Experimental Apparatus and Methods

3.1. Experimental Apparatus

Figure 1 shows the process flow diagram (PFD) of the gas injection and separation experiment to fully dissolve carbon dioxide generated after reforming hydrocarbons produced by underwater weapon systems. The experimental equipment consists of a mass flow controller (Line Tech, Daejeon, Korea) (MFC) for deciding the injection flow rate of gas, a water storage tank, a constant temperature bath for maintaining a constant water temperature inside the tank, a pump for circulating water, a porous filter for deciding the initial bubble size, an inline mixer for strengthening the turbulent flow to increase the concentration difference, a pipe for increasing the retention time, a separator for separating the dissolved gas and the undissolved remaining gas, a flow meter for measuring the undissolved gas, an instrument and control valve for controlling the process variables (pressure, temperature, and flow rate). The inner parts of the pipe and separator were flushed with N₂ gas while CO₂ was used as the experimental gas. Table 1 lists the detailed specifications of the experimental equipment.

The solvents used in this experiment were sea water and distilled water (99.9%). The artificial sea water was produced in accordance with ASTM-D1141-98 [15]. Table 2 outlines the composition of the artificial sea water used in this experiment [15].

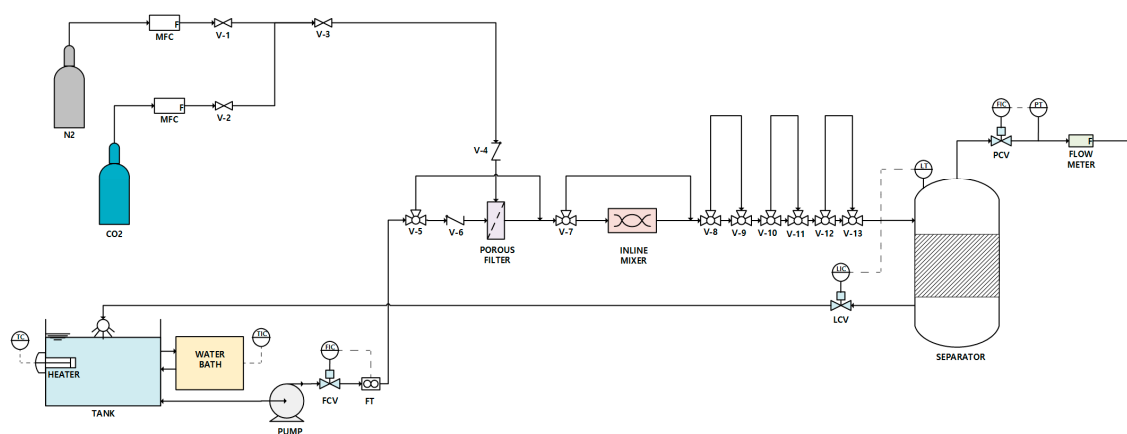


Figure 1. CO₂ injection and separation system process flow diagram (PFD).

Table 1. Specifications of equipment.

Item List	Specification
Type of Gas	N ₂ , CO ₂ (>99.9% purity)
Tank	70(W)*77(L)*68(H)
Water Bath	5–96 °C
MFC (N ₂)	0–0.25 SLPM
MFC (CO ₂)	0–25 SLPM
Pump	VFD Type
Porous Filter Grade	10 µm, 30 µm
Inline Mixer	1/2" (Clear PVC)
Pipe	40 A
Flow Control Valve	40 A, Equal%, Cv: 3.60
Pressure Control Valve	20 A, Linear, Cv: 0.02
Level Control Valve	40 A, Equal%, Cv: 2.00
Pressure Transmitter	0–10 barg
Flow Transmitter	0–25 LPM
Level Transmitter	Float Type (Resolution: 12 mm)
Flow Meter	Coriolis Type (Measurement Error Mass: 0.5%)
Separator	250 φ*1167 H (mm), Side Glass: 50 φ, Filter Grade: 300 µm

Table 2. Composition of artificial sea water.

Component	Content
NaCl	58.490%
MgCl ₂ -6H ₂ O	24.460%
Na ₂ SO ₄	9.750%
CaCl ₂	2.765%
KCl	1.645%
NaHCO ₃	0.477%
KBr	0.238%
H ₃ BO ₃	0.071%
SrCl ₂ -6H ₂ O	0.095%
NaF	0.007%

3.2. Experimental Methods

First, the system temperature is maintained at a constant 25 °C using the constant temperature tank; the pump is activated to circulate water to the separator. When the water level inside the separator becomes constant, the impurities remaining inside the pipe and separator are removed via an injection of N₂. Subsequently, the inlet flow rate of CO₂ is adjusted using the MFC and injected through the porous filter. The CO₂ inlet flow rate is 25% of the maximum quantity of CO₂ that can be dissolved in 10 L of water as determined using Henry's law. The H₂O-CO₂ mixture enters the separator through the inline mixer and pipe and is separated into dissolved gas and remaining undissolved gas. If the bubble size is smaller than 300 µm, they cannot be observed at a pressure above 2 barg. Therefore, a 300 µm mesh is installed inside the separator; bubbles larger than 300 µm escape through the top and the amount of the undissolved remaining gas is measured by the flow meter. Bubbles smaller than 300 µm escape through the bottom of the separator and return to the tank [4]. Table 3 defines the experimental case conditions.

Table 3. Case definitions.

Solvent	Distilled Water
	Sea Water
Solute	CO ₂
Temperature (°C)	25
Pressure (bara)	3
	4
Flow Rate (LPM)	Solvent: 10
	Solute: 25% of Maximum Solubility
Bubble Size (µm)	10
	30
Inline Mixer	Applied
	Not Applied
Retention Time (s)	40
	160

In this study, the effect of bubble size, turbulence intensity, and retention time on CO₂ mass transfer were evaluated. As shown in Figure 2, the experimental variables included a porous filter, inline mixer, and pipes. The filter grade of porous filter was tested to 10 and 30 µm (Figure 2a). Figure 2b shows an inline mixer for evaluating the effect of CO₂ mass transfer on the turbulence intensity. By operating the three-way valve, it was determined whether or not an inline mixer was applied. To evaluate the effect of retention time on CO₂ mass transfer, the retention time was determined using pipes as shown in Figure 2c. Retention time means the time from porous filter to separator. If no pipes were used, the retention time was 40 s, and if all pipes were passed, the retention time was 160 s.

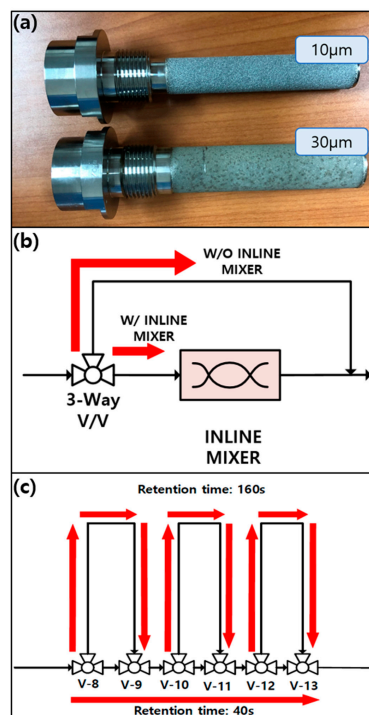


Figure 2. Experimental variables: (a) porous filter, (b) inline mixer, (c) pipes.

The rate of solution is calculated by the following equation:

$$\dot{m} = \frac{(m_{injected} - m_{residual})}{t}, \tag{7}$$

where $m_{injected}$ is the amount of injected gas and $m_{residual}$ is the amount of undissolved residual gas.

The amount of input gas is determined using the gas flow rate set in the MFC and the amount of undissolved residual gas is measured by the flow meter. The difference between these two values is then divided by the retention time to obtain the dissolution rate of the gas dissolved for the given retention time.

$$k = \frac{\dot{m}}{\pi d_b^2 (H_{CO_2} P_{CO_2} - C_{CO_2})}. \tag{8}$$

The mass transfer coefficient is derived by Equation (8), where \dot{m} is the dissolution rate obtained through experiments according to Equation (7), d_b^2 is the CO₂ bubble diameter, H_{CO_2} is the Henry's constant of CO₂, P_{CO_2} is the partial pressure of CO₂, and C_{CO_2} is the concentration of CO₂ in solvent. The experimental measurement error is lower than 8%. The experimental temperature of the carbon dioxide and the density according to the experimental pressure used for this calculation were obtained using the chemical process simulation program Aspen HYSYS V10.

4. Results and Discussions

4.1. Effect of the Bubble Size

Figure 3 compares the mass transfer coefficient according to the bubble size at different pressures. When the bubble size was 30 μm, the average mass transfer coefficient was 0.077 mm/s at 3 bara and 0.092 mm/s at 4 bara. When the bubble size was 10 μm, the average mass transfer coefficient was 0.099 mm/s at 3 bara and 0.13 mm/s at 4 bara. Thus, when the bubble size decreased from 30 to 10 μm, the average mass transfer coefficient increased by approximately 21% at the pressure of 3 bara and approximately 17% when at the pressure of 4 bara.

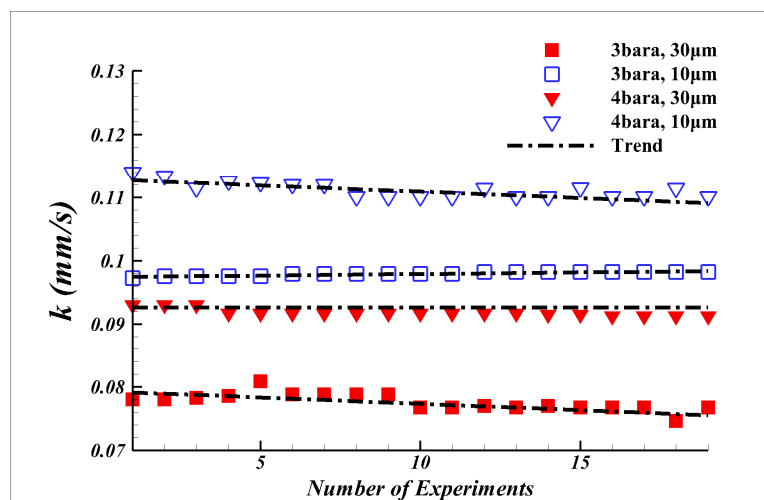


Figure 3. Comparison of mass transfer coefficients by bubble size.

This is because a smaller bubble size results in a higher number of bubbles, and the larger the contact area between the bubble and solvent becomes (Table 4).

Table 4. Number of bubbles and contact areas by bubble size.

Bubble Size	Number of Bubbles	Contact Area (mm ²)
10 μm	6.5×10^6	8204
30 μm	6.7×10^5	7606

4.2. Effect of the Turbulence Intensity

Figure 4 shows how the mass transfer coefficient changes with pressure, both when the bubble size was fixed at 30 μm and when the inline mixer was applied and when it was not.

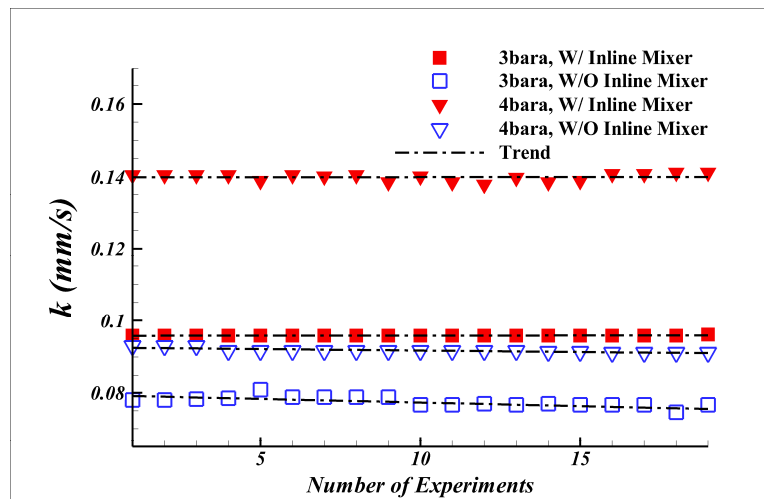


Figure 4. Comparison of mass transfer coefficients by turbulence intensity.

When the experimental pressure was 3 bara, the average mass transfer coefficient was 0.096 mm/s with the inline mixer and 0.077 mm/s without it. When the experimental pressure was 4 bara, the average mass transfer coefficient was 0.14 mm/s with the inline mixer and 0.092 mm/s without the inline mixer. Thus, the average mass transfer coefficient when the inline mixer was applied was higher by approximately 20% at the experimental pressure of 3 bara, than when it was not applied, and by approximately 34% at the experimental pressure of 4 bara. This is because the fluid was separated and the gas-liquid contact area increased when it passed through the elements inside the inline mixer; the direction of rotation changes for each element, which then forms a turbulent flow and further accelerates mass transfer. Kim et al. [16] researched how to improve the mass transfer in the process of absorbing CO₂ in a nanofluid; they found that the mass transfer coefficient increased from 5 to 11×10^4 m/s when the Reynolds number increased from 800 to 1600.

4.3. Effect of Retention Time

Figure 5 shows how the mass transfer coefficient changed when the retention times were changed to 40 and 160 s. At the experimental pressure of 3 bara, the average mass transfer coefficient was 0.077 mm/s when the retention time was 40 s and 0.029 mm/s when it was 160 s. At the experimental pressure of 4 bara, the average mass transfer coefficient was 0.092 mm/s when the retention time was 40 s and 0.036 mm/s when it was 160 s. Thus, when the retention time was increased from 40 to 160 s, the average mass transfer coefficient decreased by approximately 62% and 61% at the experimental pressures of 3 and 4 bara, respectively. When the retention time increases, the solubility also increases (Figure 6). However, the rate of solution decreases with increasing retention time because it is defined as the amount of dissolution per unit of time. Therefore, the higher the retention time, the lower the mass transfer coefficient becomes.

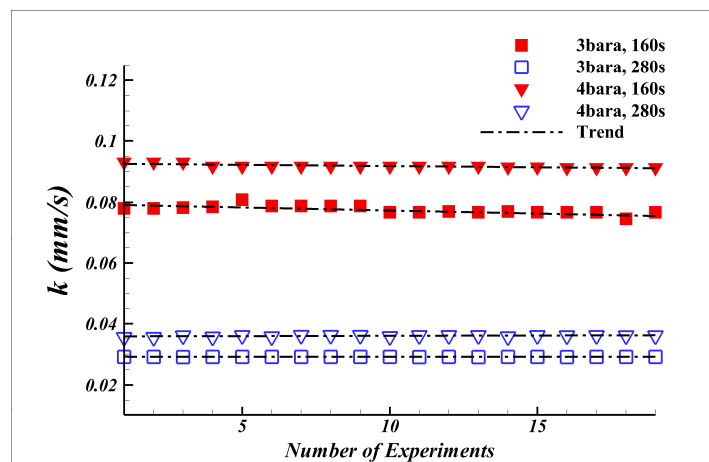


Figure 5. Comparison of mass transfer coefficients by retention time.

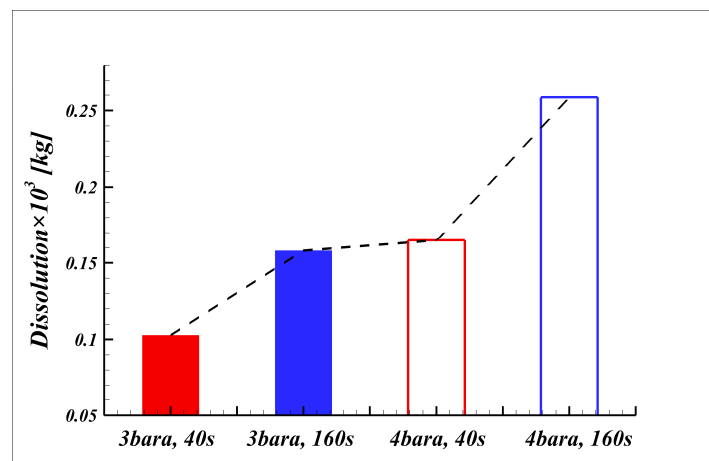


Figure 6. Comparison of dissolution by retention time.

4.4. Effect of the Solvent

Figure 7 compares the mass transfer coefficient of CO₂ between distilled water and sea water under the experimental conditions of a pressure of 3 bara, a bubble size of 30 μ m, a retention time of 40 s, and the absence of an inline mixer.

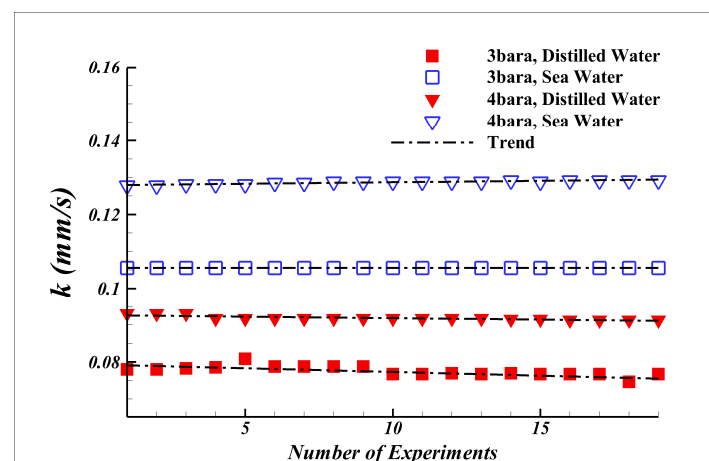


Figure 7. Comparison of mass transfer coefficients by solvent.

Under these conditions, the average mass transfer coefficient was 0.077 mm/s in distilled water and 0.11 mm/s in sea water. At an experimental pressure of 4 bara, however, the average mass transfer coefficient was 0.092 mm/s in distilled water and 0.13 mm/s in sea water. Thus, when solvent was changed to sea water, the average mass transfer coefficient increased by approximately 27% at 3 bara and by approximately 29% at 4 bara. This result contrasts those from previous studies, which show that the CO₂ diffusion coefficient is greater in distilled water than in sea water. Table 5 shows that the diffusivity and Schmidt number are different based on solvent type [9,17]. As seen in Equation (4), the mass transfer coefficient is affected by diffusivity and Schmidt number; however, the effect of the Schmidt number is greater than that of diffusivity. Therefore, the mass transfer coefficient in sea water is greater than that in distilled water.

Table 5. Diffusivity and Schmidt number by solvent.

Parameter Solvent	D (m ² /s) (Liu et al. [9])	Sc (Wanninkhof [17])
Distilled Water	1.72 × 10 ⁹	600
Sea Water	1.64 × 10 ⁹	660

4.5. Discussion

Table 6 outlines the average mass transfer coefficients of carbon dioxide in every experimental case. Among the retention time, bubble size, with (i.e., W/) or without (i.e., W/O) an inline mixer, and solvent type, the retention time had the largest effect, followed by solvent type, W/ or W/O an inline mixer, and bubble size.

Table 6. Average mass transfer coefficients for each case.

Average Mass Transfer Coefficient in Distilled Water (mm/s)								
Bubble Size	10 μm				30 μm			
Pressure	3 bara		4 bara		3 bara		4 bara	
Retention Time	40 s	160 s						
W/Inline Mixer	0.099	0.041	0.13	0.042	0.096	0.033	0.14	0.039
W/O Inline Mixer	0.098	0.030	0.11	0.035	0.077	0.029	0.092	0.036
Average Mass Transfer Coefficient in Sea Water (mm/s)								
Bubble Size	10 μm				30 μm			
Pressure	3 bara		4 bara		3 bara		4 bara	
Retention Time	40 s	160 s						
W/Inline Mixer	0.17	0.050	0.20	0.056	0.17	0.055	0.21	0.054
W/O Inline Mixer	0.14	0.037	0.16	0.047	0.11	0.050	0.13	0.051

The average mass transfer coefficient at an experimental pressure of 4 bara, bubble size of 30 μm, retention time of 160 s, and without an inline mixer was 0.036 mm/s. The average mass transfer coefficient at the experimental pressure of 3 bara, bubble size of 10 μm, retention time of 40 s, and with the inline mixer was 0.0997 mm/s. Thus, the average mass transfer coefficient increased by approximately 64% when the contact area with solvent was increased by decreasing the bubble size, reducing the retention time, and applying an inline mixer. This means that the same dissolution effect can be obtained at a high pressure and at a low pressure. Therefore, shortening the storage time of carbon dioxide in the underwater weapon system by reducing the bubble size, applying an inline mixer, and decreasing the retention time can have the same effect as reducing the size of the fuselage. However, further studies on the power requirements of the underwater weapon system are required because a pressure loss is expected due to the reduction of bubble size and the application of an inline mixer.

5. Conclusions

The mass transfer coefficients of carbon dioxide were experimentally derived while the variables affecting mass transfer were changed to discharge carbon dioxide generated from underwater weapon systems equipped with reformed fuel cells. The following conclusions were found:

1. When the bubble size decreased from 30 to 10 μm , the average mass transfer coefficient increased by -21% at the experimental pressure of 3 bara and by -17% at the experimental pressure of 4 bara. This is because the contact area between the solvent and bubble increases as the bubble size decreases.
2. When an inline mixer was applied, the average mass transfer coefficient increased by approximately 20% at the experimental pressure of 3 bara and by approximately 34% at the experimental pressure of 4 bara. This is because the inline mixer accelerates the gas–liquid mass transfer by strengthening the turbulent flow.
3. When the retention time increased from 40 to 160 s, the average mass transfer coefficient decreased by -62% at the experimental pressure of 3 bara and -61% at the experimental pressure of 4 bara. This is because when the retention time increases, the dissolution amount increases, but the rate of solution decreases because the rate of solution is defined by the dissolution amount per time.
4. When the solvent type was changed to distilled water and sea water, the average mass transfer coefficient in the distilled water was lower by -27% at the experimental pressure of 3 bara and -29% at the experimental pressure of 4 bara. This is because the change rate of Schmidt number according to the change of solvent is larger than the change rate of diffusivity.
5. The same effect as dissolution at a high pressure can be obtained at a low pressure by reducing the bubble size, increasing the retention time, and applying the inline mixer. Thus, it is expected that shortening the time that carbon dioxide is stored in the underwater weapon system will reduce the size of the underwater weapon system.
6. Future studies on the increased power requirements of the underwater weapon system should be made because a pressure loss is expected due to the reduction of bubble size and the application of an inline mixer.

Author Contributions: Supervision, J.C.; Methodology, J.C. and H.-J.C.; Investigation, J.C. and H.-J.C.; Funding acquisition, J.C.; Writing—Review and editing, J.C. and H.-J.C.

Funding: This research was funded by Defense Acquisition Program Administration.

Acknowledgments: This research is part of the work supported by the Defense Acquisition Program Administration and the Agency for Defense Development. [Project Name: 17-113-407-039].

Conflicts of Interest: The authors declare no conflict of interest.

References

1. Yin, B.; Zou, Y.; Wang, J. Studies on New High-Effective Power System of Conventional Submarine. In Proceedings of the Sixth International Conference on Electrical Machines and Systems, Beijing, China, 9–11 November 2003; pp. 923–925.
2. De-Troya, J.J.; Alvarez, C.; Fernández-Garrido, C.; Carral, L. Analysing the Possibility of Using Fuel Cells in Ships, International. *J. Hydrog. Energy* **2016**, *41*, 2853–2866. [[CrossRef](#)]
3. Daniel, R.P.; Robert, A.D.; Jamie, D.H. Methanol Steam Reforming for Hydrogen Production. *J. Am. Chem. Soc.* **2007**, *107*, 3992–4020.
4. Stefan, K.; Javier, L. Methanol Reformer—The Next Milestone for Fuel Cell Powered Submarines. *Int. J. Hydrog. Energy* **2015**, *40*, 5482–5486.
5. Noorlisa, H.; Thanita, N.; Peter, L.D.; Eric, C.; Luis, A.R.-S. Dynamic Simulation of MEA Absorption Process for CO₂ Capture from Power Plants. *Int. J. Greenh. Gas Control* **2012**, *10*, 295–309.
6. Chen, P.C.; Huang, C.H.; Su, T.; Chen, H.W.; Yang, M.W.; Tsao, J.M. Optimum Condition for the Capture of Carbon Dioxide with a Bubble-Column Scrubber. *Int. J. Greenh. Gas Control* **2015**, *35*, 47–55. [[CrossRef](#)]

7. Abu-Zahra, M.R.; Schneiders, L.H.; Niederer, J.P.; Feron, P.H.; Versteeg, G.F. CO₂ Capture from Power Plant: Part 1. A Parametric Study of the Technical Performance Based on Monoethanolamine. *Int. J. Greenh. Gas Control* **2007**, *1*, 37–46. [[CrossRef](#)]
8. Calderbank, P.H.; Lochiel, A.C. Mass Transfer Coefficient, Velocities and Shapes of Carbon Dioxide Bubbles in Free Rise Through Distilled Water. *Chem. Eng. Sci.* **1964**, *19*, 485–503. [[CrossRef](#)]
9. Liu, Q.; Endo, H.; Fukuda, K.; Shibahara, M.; Zhang, P. Experimental Study on Solution and Diffusion Process of Single Carbon Dioxide Bubble in Seawater. *Mech. Eng. J.* **2016**, *3*, 1–9. [[CrossRef](#)]
10. Jan, E.O.; Dorien, D.; Emlyn, D.; Paal, S.; John, M. Mass Transfer Between Bubbles and Seawater. *Chem. Eng. Sci.* **2017**, *161*, 308–315.
11. Ranz, W.E.; Marshall, W.R.J. Evaporation from Droplets Parts I & II. *Chem. Eng. Prog.* **1952**, *48*, 173–180.
12. Leifer, I.; Patro, R.K. A Review and Sensitivity study. *Cont. Shelf Res.* **2002**, *22*, 2409–2428. [[CrossRef](#)]
13. Ng, W.Y.; Walkley, J. Diffusion of Gases in Liquids: The Constant Size Bubble Method. *Can. J. Chem.* **1969**, *47*, 1075–1077. [[CrossRef](#)]
14. Higbie, R. The rate of absorption of a pure gas into a still liquid during short periods of exposure. *Trans. AIChE* **1935**, *31*, 365–389.
15. ASTM. *D1141-98: Standard Practice for The Preparation of Substitute Ocean Water*; American Society for Testing and Materials International: West Conshohocken, PA, USA, 2013.
16. Kim, J.H.; Jung, C.W.; Kang, Y.T. Mass Transfer Enhancement during CO₂ Absorption Process in Methanol/Al₂O₃ Nanofluids. *Int. J. Heat Mass Transf.* **2014**, *76*, 484–491. [[CrossRef](#)]
17. Rik, W. Relationship Between Wind Speed and Gas Exchange Over the Ocean. *J. Geophys. Res.* **1992**, *97*, 7373–7382.



© 2019 by the authors. Licensee MDPI, Basel, Switzerland. This article is an open access article distributed under the terms and conditions of the Creative Commons Attribution (CC BY) license (<http://creativecommons.org/licenses/by/4.0/>).